

Charged-pion correlations caused by chiral relaxation dynamics in high-energy nuclear collisions

Jørgen Randrup

Nuclear Science Division, Lawrence Berkeley National Laboratory, 1 Cyclotron Road, Berkeley, California 94720

(Received 2 January 2002; published 29 April 2002)

For cylindrical systems endowed with a longitudinal Bjorken scaling expansion, the semiclassical linear sigma model is employed to calculate the self-consistent dynamical evolution from the initially hot configuration towards the asymptotic state of freely moving pions. The correlation function for charge-conjugate soft pions with similar rapidities and transverse energies exhibits pronounced azimuthal anticorrelations that may be used to probe the nonequilibrium chiral relaxation dynamics.

DOI: 10.1103/PhysRevC.65.054906

PACS number(s): 25.75.Dw, 25.75.Gz, 11.30.Rd

I. INTRODUCTION

It was recently suggested that the nonequilibrium relaxation dynamics of the chiral order parameter in a high-energy nuclear collision may give rise to the production of approximately back-to-back charge-conjugate pairs of soft pions [1]. The basic production mechanism behind this effect is the rapid but quasiregular change of the produced medium, as manifested in the time dependence of the effective pion mass. This time dependence produces charge-conjugate pion pairs that, insofar as the environment varies relatively gently in space, carry only rather little total momentum.

If this signal indeed appears at an experimentally discernible level, the effect might provide a novel means for probing chiral symmetry far away from the familiar region near the ordinary vacuum. The purpose of the present paper is to examine the effect on the basis of more refined numerical calculations. The presentation first puts the issue into the context of the current high-energy heavy-ion efforts and explains the general features of the effect. Subsequently, the semiclassical linear σ model is employed for rodlike systems endowed with a longitudinal Bjorken expansion. Finally, the prospects for the practical observation of the effect are discussed.

Nuclear collision experiments at high energy offer the prospect of exploring the phase diagram for strongly interacting matter. The violent collision of the two nuclei produces a spatially extended region within which the energy density exceeds that required for (effective) quark deconfinement and (approximate) chiral-symmetry restoration. One may then expect that the magnitude of the chiral order parameter inside the agitated region is significantly reduced relative to its vacuum value of $f_\pi \approx 92$ MeV. Therefore, such collisions may provide a means for probing the chiral features far away from the ordinary vacuum and thus help advance our understanding of this important symmetry.

The produced highly agitated region is expanding rapidly, at first primarily in the longitudinal direction, due to the large momentum of the colliding nuclei, but then gradually in the transverse directions as well. It has been speculated that such a rapid expansion of the collision zone, after the approximate restoration of chiral symmetry has occurred, may produce long-wavelength isospin-polarized agitations of the pionic

field, commonly referred to as disoriented chiral condensates, as reviewed in Refs. [2–4].

In the idealized case when all observed pions arise from a single fully polarized source, the neutral pion fraction f (the number of neutral pions divided by the total pion number) would have an anomalous form, $P(f) = 1/2\sqrt{f}$. This prospect stimulated experimental efforts to search for a broadening in $P(f)$ but they yielded a null result [5,6]. Subsequently, less idealized model calculations have suggested that any such effect is carried primarily by relatively soft pions and may only be visible if the analysis is limited to those [7]. However, such an undertaking is hampered by the difficulty of reconstructing the individual speeds of the neutral pions from the observed photons. Consequently, the neutral pion fraction appears to be a less suitable observable.

Fortunately, the nonequilibrium chiral dynamics may also manifest itself in observables based exclusively on charged pions, which can be observed individually with good kinematical resolution. Thus, relatively recent numerical simulations with the semiclassical linear σ model have identified a number of candidate observables [8]. Most basically, the soft pions arising from the relaxation dynamics of the chiral order parameter may lead to a marked enhancement in the transverse spectral profile below $p_\perp \approx 200$ MeV/c. Moreover, the associated multiplicity is expected to exhibit anomalous fluctuations. While a spectral enhancement by itself would be less specific, due to the presence of other sources of soft pions, the anomalous multiplicity correlation appears more promising since the effect was shown to be absent in the commonly used UrQMD [9] and HIJING [10] event generators that involve conventional physics only [11].

Even more experimentally attractive is the recently suggested back-to-back correlation between oppositely charged soft pions [1] and we report here on more detailed studies of this candidate signal, carried out within the calculational framework employed in Ref. [8].

Before moving on to the task at hand, it may be instructive to briefly make contact with other current attempts to use charged-pion fluctuations as probes in high-energy nuclear collisions. In particular, Jeon and Koch [12] recently considered the possibility of using the event-by-event fluctuation of the ratio of positive and negative pions as a means for distinguishing between the confined and the deconfined phases, the idea being that the smaller constituent charges in

the quark-gluon plasma will reduce the relative charge fluctuations. A similar study was made by Asakawa *et al.* [13] who also considered fluctuations in the baryon number. This type of observable is based on the imbalance of the number of positive and negative pions (or baryons and antibaryons) within a given volume (in practice characterized by a certain rapidity interval), while the specific spectral distributions and angular correlations are unessential for the purpose. In a conceptually different approach, Bass *et al.* [14] consider the balance functions, that give the conditional probability that a hadron h having the rapidity y_1 is accompanied by a corresponding antiparticle \bar{h} with a different rapidity y_2 . This type of correlation information may be used to clock the hadronization, since the charge-conjugate hadron pairs produced by the hadronization emerge as ever more tightly correlated in rapidity the later they are formed. Again, the specific spectral distributions and angular correlations are not utilized.

II. CALCULATIONAL DETAILS

Considerable insight into the chiral relaxation dynamics can be gained from the linear σ model. In order to make actual numerical simulations possible, we shall treat the model at the classical level so that the dynamical variable is $O(4)$ chiral field strength $\phi = (\sigma, \pi)$, which consists of the isoscalar $\sigma(\mathbf{r})$ field and the isovector pion field $\pi(\mathbf{r})$.

For uniform systems in thermal equilibrium, a Hartree-type factorization reduction leads to a separation of the field into an $O(4)$ order parameter and approximately independent quasiparticle modes characterized by a common $O(4)$ effective-mass tensor. By populating these modes according to quantum statistics, one obtains the semiclassical linear σ model [15]. Nonuniform initial geometries can be constructed subsequently by suitable manipulation of such basic thermal fields [7,8].

Once initialized, the chiral field evolves according to the equation of motion,

$$[\square + \lambda(\phi \circ \phi - v^2)]\phi = H e_\sigma, \quad (1)$$

where \circ is the scalar product in the $O(4)$ chiral space and the unit vector e_σ points in the σ direction. In order to emulate the effect of the rapid longitudinal expansion of the source produced in a high-energy nuclear collision, we consider systems endowed with a scaling expansion of the Bjorken type. The continual stretching in the beam direction can be absorbed by replacing the standard Cartesian coordinates (x, y, z, t) by the comoving variables (x, y, η, τ) ,

$$z = \tau \sinh \eta, \quad t = \tau \cosh \eta, \quad (2)$$

thus making the numerical treatment tractable. The local reference frame then moves with the rapidity η and τ is the associated proper time. We note that $dzdt = \tau d\eta d\tau$ and that the d'Alembert operator is modified,

$$\partial_t^2 - \partial_z^2 = \frac{1}{\tau} \partial_\tau \tau \partial_\tau - \frac{1}{\tau^2} \partial_\eta^2 = \partial_\tau^2 + \frac{1}{\tau} \partial_\tau - \frac{1}{\tau^2} \partial_\eta^2. \quad (3)$$

Thus the longitudinal stretching introduces a damping term that causes the local field amplitude to exhibit an overall decrease in time (see below).

A. Initialization

Since the numerical treatment is identical to what was already described in Ref. [8], we need only recall the main features here. The chiral field is represented on a rectangular lattice in position space. In order to construct the initial field configuration, the field strength at each lattice site, $\phi(x, y, z)$, and the associated time derivatives $\psi(x, y, z)$, are sampled from a thermal ensemble characterized by a specified initial source temperature T_0 , using the method developed in Ref. [15]. This field configuration would constitute an appropriate initial condition for a uniform and nonexpanding system. It can be adapted to Bjorken-type scenarios by simply replacing the longitudinal coordinate z by variable η (and the initial time t_0 by τ_0). [It may be noted that the statistical ensemble of initial states is isotropic with respect to isospin (implying that the expected quasiparticle mode occupancies are independent of the pionic charge ν) and, importantly, it contains no correlations between those modes, apart from the Bose-Einstein autocorrelations dictated by quantum statistics. Therefore, any final correlation between positive and negative pions has been dynamically generated.]

Subsequently, a rodlike configuration is generated by suitable (and spatially smooth) modulation of the field components outside a circular disk in the transverse plane, as described in Ref. [8]. With ρ denoting the transverse position (x, y) , the resulting field configuration, $[\phi(\rho, \eta), \psi(\rho, \eta)]$, then describes a “Bjorken rod” at the initial proper time τ_0 . Being endowed with a Bjorken expansion in the longitudinal direction, the system has a circular cross section and the field strength appears locally as if sampled from a thermal ensemble having a temperature $T(\rho)$ that falls off from T_0 in the interior towards zero in accordance with a specified diffuse (folded-Yukawa) profile function. The associated transverse radius is denoted by R_0 . In the limit of large rod radii, $R_0 \rightarrow \infty$, the system approaches that of “Bjorken matter,” a spatially uniform system endowed with the longitudinal Bjorken expansion.

It is important to appreciate that the term “uniform” refers to the *macroscopic* appearance of the system and is not meant to suggest that the field strength is independent of position; locally the field varies rapidly but in a manner that is statistically similar everywhere. In a similar manner, the Bjorken rod is uniform along the longitudinal direction, reflecting the intended macroscopic boost invariance. These ensemble invariances are preserved in the course of the dynamical evolution.

B. Asymptotic analysis

Once the field has been initialized, its temporal evolution may be determined by solving the field equation with a simple leapfrog method. For the present purposes we need to be concerned only with the behavior of the pion field at large times, $\pi(\rho, \eta, \tau \rightarrow \infty)$.

While the numerical treatment is most conveniently carried out in terms of the Cartesian components of the pion field (which are real), $\pi^{(j)}$, $j=1,2,3$, the observed pions have a definite charge, $\nu=-,0,+$, and so they are represented by the spherical components π^ν ,

$$\pi^\pm = \frac{1}{\sqrt{2}} [\pi^{(1)} \pm i\pi^{(2)}], \quad \pi^0 = \pi^{(3)}. \quad (4)$$

Due to the cylindrical geometry of the rod system, it is useful to represent the pion field as follows:

$$\pi(\boldsymbol{\rho}, \eta) = \frac{1}{L} \sum_{\mathbf{k}} \pi_{\mathbf{k}}(\eta) e^{i\mathbf{k} \cdot \boldsymbol{\rho}}, \quad (5)$$

where L is the side length of the numerical lattice in the x and y directions and \mathbf{k} is the transverse wave vector.

At large times $\tau \gg \tau_0$, the equation of motion for the mixed transform simplifies,

$$\left[\partial_\tau^2 + \frac{1}{\tau} \partial_\tau + m_k^2 \right] \pi_{\mathbf{k}}^\nu(\eta) = \mathcal{O}\left(\frac{\tau_0^2}{\tau^2}\right), \quad (6)$$

where the transverse mass is given by $m_k^2 = m_\pi^2 + k^2$. The field transforms $\pi_{\mathbf{k}}^\nu(\eta)$ are thus of Bessel form and subside as $1/\sqrt{\tau}$. This attenuation is a result of the continual Bjorken stretching that endows the pion frequency with an imaginary part, $\omega_k \approx m_k - i/2\tau$, so we have

$$\pi_{\mathbf{k}}^\nu(\eta) \sim \exp\left[-i \int^\tau d\tau' \omega_k(\tau')\right] \sim \frac{1}{\sqrt{\tau}} e^{-im_k \tau}. \quad (7)$$

In this limit, we may extract the following key quantity:

$$\chi_{\mathbf{k}}^\nu(\eta) = \sqrt{\tau} \left[\sqrt{\frac{m_k}{2}} \pi_{\mathbf{k}}^\nu(\eta) + \frac{i}{\sqrt{2m_k}} \dot{\pi}_{\mathbf{k}}^\nu(\eta) \right], \quad (8)$$

which expresses the amplitude for the final state to contain pions of charge ν having the transverse momentum \mathbf{k} and being longitudinally located at η (hence moving with the rapidity $y = \eta$). Then the number of pions with the specified ν and \mathbf{k} emitted within a specified rapidity interval (y_1, y_2) is readily expressed,

$$N_{\mathbf{k}}^\nu(y_1, y_2) = \int_{y_1}^{y_2} d\eta |\chi_{\mathbf{k}}^\nu(\eta)|^2. \quad (9)$$

The appearance of the proper time τ in the expression (8) for the pion amplitude is a reflection of the longitudinal expansion and it compensates for the steady decrease of the amplitude, thus ensuring that the extracted results are insensitive to τ and hence numerically robust.

C. Event sampling

In order to emulate the experimental event sampling, we prepare a sample of \mathcal{N} different initial field configurations, constructed as explained above, and then analyze the asymptotic results of the ensuing \mathcal{N} dynamical histories. The

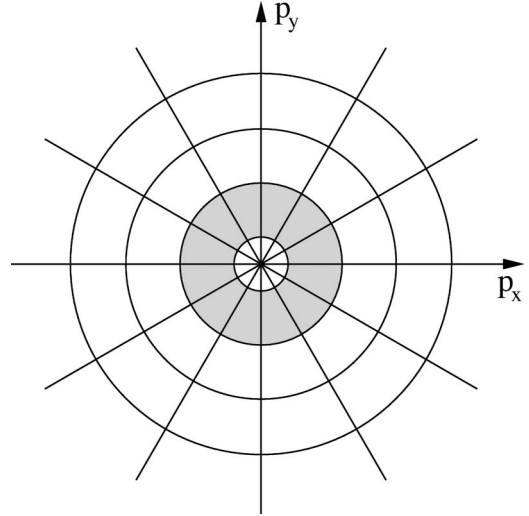


FIG. 1. Illustration of the sampling bins employed for the transverse pion momenta \mathbf{k} , for the standard case of $N_\varphi = 12$ azimuthal sectors of 30° (see the text for details).

statistical fluctuations from one initial field to the next leads to corresponding event-by-event fluctuations in the extracted amplitudes $\chi_{\mathbf{k}}^\nu(\eta)$ and hence in the values $N_{\mathbf{k}}^\nu(y_1, y_2)$. The expected multiplicity density for pions of charge ν and transverse momentum \mathbf{k} emitted within the given rapidity interval is then obtained by averaging over the event sample,

$$\left\langle \frac{dN_{\mathbf{k}}^\nu}{dy} \right\rangle = \frac{1}{\mathcal{N}} \sum_{n=1}^{\mathcal{N}} \frac{1}{\Delta y} N_{\mathbf{k}}^{\nu;n}(y_1, y_2), \quad (10)$$

with each “event” being labeled by the index n and with $\Delta y = y_2 - y_1$ denoting the width of the rapidity interval.

It takes three kinematical variables to characterize the final state of a pion (rapidity y , transverse mass m_k , and azimuthal angle φ). Then the two-pion correlation function will depend on six kinematical variables and hence it is difficult to display and analyze. We, therefore, prefer to reduce the information by suitable binning.

For our present purposes, it is instructive to bin the transverse momentum \mathbf{k} according to transverse mass m_k and azimuthal angle φ . In order to simplify the presentation, we shall consider only a few relatively wide energy bands (labeled by m) and N_φ equal-size angular sectors (labeled by ι), as illustrated in Fig. 1.

Furthermore, we consider N_l rapidity “lumps” of equal size Δy (labeled by l). Due to the boost invariance of the ensemble, these lumps are calculationally equivalent, which effectively increases the sample size by a factor of N_l . A given event n then emits $N_{lm\iota}^{\nu;n}$ charge- ν pions into the kinematical domain identified by the labels (l, m, ι) and the corresponding sample-averaged multiplicity is

$$\langle N_{lm\iota}^\nu \rangle = \frac{1}{\mathcal{N}} \sum_{n=1}^{\mathcal{N}} N_{lm\iota}^{\nu;n} = N_m. \quad (11)$$

Here the last expression exploits the symmetries with respect to ν , l , and ι , which imply that the ensemble average depends only on the transverse mass m_k ,

$$N_m = \frac{1}{3} \sum_{\nu=-1}^1 \frac{1}{N_l} \sum_{l=1}^{N_l} \frac{1}{N_\varphi} \sum_{\varphi=1}^{N_\varphi} \langle N_{lm\nu}^\nu \rangle. \quad (12)$$

In order to keep the two-particle information to a manageable level, we examine only those pion pairs for which both partners emerge within the same rapidity lump l and in the same energy band m . For each such bin in rapidity and transverse mass, the two-particle correlation depends on the two azimuthal angles φ and φ' (and on the charges ν and ν'),

$$\begin{aligned} \sigma_{lm;\nu\nu'}^{\nu\nu'} &= \langle N_{lm\nu}^\nu N_{lm\nu'}^{\nu'} \rangle - \langle N_{lm\nu}^\nu \rangle \langle N_{lm\nu'}^{\nu'} \rangle \\ &= \frac{1}{N} \sum_{n=1}^N N_{lm\nu}^{\nu;n} N_{lm\nu'}^{\nu';n} - \left(\frac{1}{N} \sum_{n=1}^N N_{lm\nu}^{\nu;n} \right) \left(\frac{1}{N} \sum_{n=1}^N N_{lm\nu'}^{\nu';n} \right). \end{aligned} \quad (13)$$

Since all the rapidity lumps l are equivalent, we may subsequently average over those, $\sigma_{m;\nu\nu'}^{\nu\nu'} = \sum_l \sigma_{lm;\nu\nu'}^{\nu\nu'} / N_l$. Furthermore, the rotational symmetry in the transverse plane implies that this quantity depends only on the angular difference $\Delta\varphi = \varphi - \varphi'$, yielding $\sigma_m^{\nu\nu'}(\Delta\varphi)$ (in fact, it depends only on the absolute difference $|\Delta\varphi|$).

The quantity $\sigma_m^{\nu\nu'}(\Delta\varphi)$ expresses the correlation between the concurrent appearance of a charge- ν pion in the bin $lm\nu$ and a charge- ν' pion in the bin $lm\nu'$, after averaging over l and binning according to $\Delta\varphi$. To further simplify the analysis, we concentrate on the situations where the two charges are either equal (Eq) or opposite (Op) and we divide by the average uncorrelated background to bring forth the relative strength of the signal,

$$C_m^{\text{Eq}}(\Delta\varphi) = \frac{1}{2} N_m^{-2} [\sigma_m^{++}(\Delta\varphi) + \sigma_m^{--}(\Delta\varphi)], \quad (14)$$

$$C_m^{\text{Op}}(\Delta\varphi) = \frac{1}{2} N_m^{-2} [\sigma_m^{+-}(\Delta\varphi) + \sigma_m^{-+}(\Delta\varphi)]. \quad (15)$$

We denote these as the *reduced* correlation functions.

III. RESULTS AND DISCUSSION

After the above brief description of the most relevant calculational details, we turn now to the extracted results for the pion correlation function.

The primary purpose of the present investigation is to achieve an impression of the magnitude of the expected correlation signal under more realistic circumstances than those considered originally in Ref. [1], where the effect was illustrated by means of a quantum-field treatment in a one-dimensional effective-mass scenario, with the mass being either constant in space or having a folded-Yukawa profile. We consider here a Bjorken rod, which presents a scenario that is more realistic in several regards: (1) the system is fully three dimensional, (2) it is in a state of rapid longitudinal expansion, and (3) it has a finite transverse extension. Moreover, we initialize and propagate the field by means of the semi-classical linear σ model, so the self-interaction of the field is retained rather than approximated in terms of an effective mass.

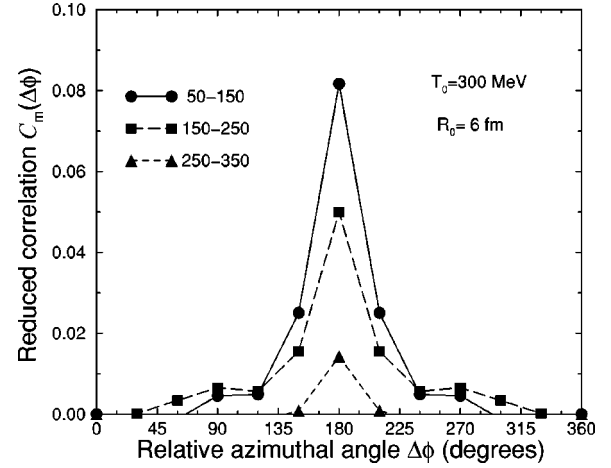


FIG. 2. The reduced azimuthal correlation function $C_m^{\text{Op}}(\Delta\varphi)$ given in Eq. (15) for oppositely charged pions resulting from a Bjorken rod with $R_0 = 6$ fm and $T_0 = 300$ MeV, for the first several transverse-momentum bands of width 100 MeV/c. The azimuthal sector width is 30° (as illustrated in Fig. 1), and the symbols are placed at the corresponding section centers.

A. Bjorken rods

To provide a specific focus for the discussion, we consider first a Bjorken rod with an initial transverse radius of $R_0 = 6$ fm and an initial central temperature of $T_0 = 300$ MeV. The resulting reduced azimuthal correlation function for oppositely charged pions is shown in Fig. 2 for the first several energy bands.

Several features are noteworthy. It is evident that the softest pions indeed exhibit a significant correlation that is concentrated in the back-to-back direction. Furthermore, not only does the signal itself grow larger as the energy is reduced, but the azimuthal width increases as well. Such an evolution is expected on general grounds, since the softest pions are affected the most by the presence of the surface. For transverse momenta around 100 MeV/c, the peak around $\Delta\varphi = 180^\circ$ has a full width at half maximum of $\approx 90^\circ$, corresponding to a dispersion of $\approx 40^\circ$ in the azimuthal correlation function. While this width is sufficiently large to render the calculated result insensitive to the number of azimuthal sectors employed, and thus numerically robust, it is at the same time sufficiently small to facilitate its extraction from the data. For the higher energy bands the antialignment is more perfect, with the correlation function being practically concentrated in the single angular bin corresponding to $\Delta\varphi = 180^\circ$. These features are consistent with our general expectation that the harder pions are less deflected by the surface.

The results depend both on the radius of the initial rod configuration and on its central temperature, but the results of the various scenarios have the same qualitative appearance. We may, therefore, illustrate these dependences by considering just the peak values at $\Delta\varphi = 180^\circ$.

The dependence on the geometry is illustrated in Fig. 3, that shows the back-to-back correlation as a function of transverse momentum p_T for both the sample of Bjorken rods leading to Fig. 2 and for a corresponding sample of

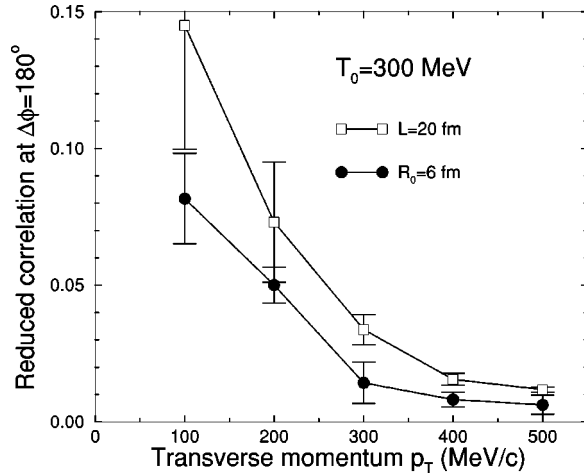


FIG. 3. The value of the reduced azimuthal pion correlation function at $\Delta\phi=180^\circ$ for a sample of Bjorken rods (solid circles) with an initial bulk temperature of $T_0=300$ MeV and an initial radius of $R_0=6$ fm and for a corresponding sample of Bjorken boxes with the same T_0 and a transverse side length of $L=20$ fm. There are 12 azimuthal sectors of 30° and the points are located at the center of each momentum band (of width 100 MeV/c).

“Bjorken box” configurations. (A Bjorken box is similar to a Bjorken rod with regard to the longitudinal expansion but it is uniform also in the transverse plane, with periodic boundary conditions.) The dependence on transverse momentum of the back-to-back correlation coefficient for the box configuration is seen to be qualitatively similar to the result for the rod and the display brings out the concentration of the effect towards the soft end of the spectrum.

The box geometry has no surface through which particles can be emitted and free pions may appear only at late times as a result of the dilution induced by the Bjorken stretching. Furthermore, there are no surface gradients present to erode the correlation between the produced pairs. However, despite the macroscopic uniformity of the system, the Hamiltonian does not decouple, due to the interaction term. Consequently, the produced (quasi)pions may still be rescattered in the medium and so they will generally not remain degenerate and oppositely moving. The numerical results suggest that this effect is relatively insignificant and the back-to-back correlation of the produced pairs thus remains largely intact. In fact, the rescattering is relatively unimportant compared to the smearing caused by the rather crude binning employed in the present illustrative analysis. This suggests that the signal may be enhanced by employing more carefully designed kinematical cuts.

To elucidate the temperature dependence of the correlation signal, we consider first Table I that shows how various characteristic quantities depend on T_0 . Generally, the chiral order parameter σ_0 becomes steadily smaller as the temperature is raised (though perfect chiral symmetry is never achieved since the finite quark mass introduces a bias in the σ direction and causes the minimum of the free energy to always lie on the positive part of the σ axis in the $O(4)$ space of the order parameter). In concert with this evolution, the effective pion mass increases steadily. The corresponding

TABLE I. Characteristic quantities for a range of central rod temperatures T_0 (MeV): the equilibrium value of the chiral order parameter σ_0 (MeV), the associated effective pion mass μ_0 (MeV/c²), the energy density ϵ_0 (MeV/fm³), the density of quasipions ρ_0 (fm⁻³), the occupancy f_0 of the lowest quasiparticle mode ($k=0$), and the approximate final rapidity density of free pions for a rod with $R_0=6$ fm.

T_0	σ_0	μ_0	ϵ_0	ρ_0	f_0	dN/dy
200	61.6	236	191	0.26	0.42	26
220	42.2	245	305	0.35	0.49	41
240	27.0	272	433	0.45	0.47	56
270	17.0	326	652	0.60	0.43	80
300	12.6	380	920	0.78	0.39	106
350	8.2	466	1485	1.12	0.36	150
400	6.2	544	2191	1.52	0.34	200

energy density of the medium increases rapidly with temperature, while the density ρ_0 of the medium-modified pions (the quasiparticles) increases at a more moderate rate, since their mass is increasing as well. As a consequence, the corresponding quasiparticle gas, in fact, becomes somewhat more dilute through this temperature range, as reflected in the decrease of the occupation coefficient f_0 for the lowest quasiparticle mode (having $k=0$). The final rapidity density of free pions, dN/dy , is determined by the dynamical history. It increases steadily with T_0 and is, of course, roughly proportional to the initial cross section of the system, πR_0^2 , but it generally remains significantly below the observed values, as will be addressed later.

Figure 4 shows how the back-to-back correlation coefficient depends on the initial temperature T_0 . Obviously, the effect disappears as the initial temperature is decreased, since

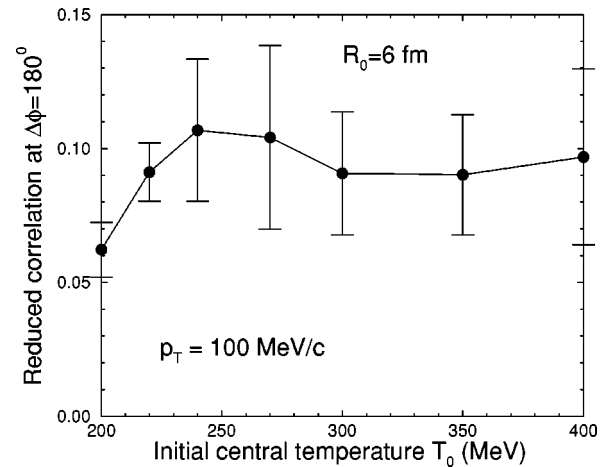


FIG. 4. The back-to-back ($\Delta\phi=180^\circ$) value of the reduced azimuthal pion correlation function for the first transverse-momentum band around $p_T=100$ MeV/c is shown as a function of the initial central temperature $T_0=300$ MeV in a sample of Bjorken rods with $R_0=6$ fm. The error bars reflect the statistical fluctuations in the value extracted for the different (but equivalent) rapidity lumps.

the initial order parameter then approaches the vacuum value f_π and, consequently, the ensuing relaxation becomes ever gentler. After its initial steady rise below the chiral transition temperature $T_\chi \approx 230$ MeV [15,16] the peak strength levels off at nearly 10% and remains rather insensitive to T_0 from thereon.

B. Observability

Although the calculated signal magnitude of 8–10 % sounds observationally attractive, as it would be easily identifiable, it should not be taken at face value. In particular, it is important to recognize that the linear σ model includes only a limited number of degrees of freedom and, accordingly, it significantly underestimates the total pion yield (see Table I). It is, therefore, to be expected that a more complete calculation, not yet available, would degrade the signal considerably. This is partly because of the additional uncorrelated background (approximately by a factor of the square of the ratio between the presently calculated yield of soft pions and the observed one, easily an order of magnitude or more) and partly because of possible direct collisions between the signal pions and those of the environment, as briefly discussed below.

Furthermore, when extracting the reduced correlation function (15), it may advisable to divide by the actual yield of the specified kind of pion in the particular angular sector, rather than by the average, since the detection efficiency may depend on both angle and charge. Thus, the reduced correlation function (15) may be extracted as follows:

$$C_{m;\iota,\iota'}^{\text{Op}} = \frac{1}{2} \left[\frac{\langle N_\iota^+ N_{\iota'}^- \rangle}{\langle N_\iota^+ \rangle \langle N_{\iota'}^- \rangle} + \frac{\langle N_\iota^- N_{\iota'}^+ \rangle}{\langle N_\iota^- \rangle \langle N_{\iota'}^+ \rangle} \right] - 1, \quad (16)$$

where N_ι^ν denotes the number of charge- ν pions in the angular sector ι with a transverse energy within the band m . The result can then be subsequently binned according to the azimuthal difference between the sectors, $\Delta\varphi$.

When trying to assess the practical visibility of the signal, one needs to take account of the sizable background contribution from pion sources not taken into account in the linear σ model. Insofar as those additional sources are devoid of specific back-to-back charge-conjugate pairs of soft pions, their effect may be approximately accounted for by renormalizing the calculated relative correlation by the product of the corresponding multiplicity ratios, yielding

$$\tilde{C}_m^{\text{Op}}(\Delta\varphi) = \frac{N_m^+(\text{L}\sigma\text{M})}{N_m^+(\text{obs})} \frac{N_m^-(\text{L}\sigma\text{M})}{N_m^-(\text{obs})} C_m^{\text{Op}}(\Delta\varphi), \quad (17)$$

where $N_m^\nu(\text{L}\sigma\text{M}) = N_m^\nu$ is the calculated rapidity density of charge- ν pions in the energy band m [see Eq. (11)], while $N_m^\nu(\text{obs})$ is the corresponding observed quantity (approximately equal to what would result from a more complete model, such as UrQMD [9] or HIJING [10]). Such comparisons indicate that here the underprediction in the soft region

of interest may well amount to a factor of three, or more, thus easily reducing the expected correlation signal by an order of magnitude.

Potentially more problematic is the possible degradation of the primary signal while the produced pions propagate within the interaction zone (since those pions are soft they might easily be deflected by encounters with other hadrons present). A rough feeling for the importance of such collisions may be obtained by noting that if the survival chance of a given signal pion is P_0 (the probability that a produced signal pion avoids significant deflection on its way out) then the correlation signal (17) is degraded by the corresponding square, P_0^2 , so that a 50% survival chance would degrade the signal by a factor of 4. Fortunately, the very mechanism by which the signal pions are produced, the oscillatory relaxation of the chiral order parameter, guarantees that they appear only relatively late. Simple estimates, as well as more elaborate numerical studies [17], show that it takes several to many fm/c for the amplification mechanism to complete (say 5 fm/c). At this time, most of the material in the collision zone has already dispersed, so the pions of interest will be born in a relatively dilute environment and, being soft, they will be too slow to catch up with already emitted particles. It would obviously be interesting to carry out a quantitative study of this delicate issue whenever a more complete model becomes available.

One might also be concerned about the possible presence of other agencies that may lead to a similar signal and thus obscure the signal of interest, but a closer analysis suggests that there may not be any serious contenders. It is particularly important to discuss the dominant decay of the relatively abundant $\rho(770)$, $\rho \rightarrow \pi^+ \pi^-$. Although the two pions are back-to-back correlated, they emerge from a ρ meson at rest with momenta of about 360 MeV/c, which is somewhat above the upper limit of the expected effect ($p_{\text{max}} \approx 200$ MeV/c). (While the decay of a ρ meson in motion may well contribute a single pion to the yield below this limit, the contribution to the coincidence yield is insignificant even when the final ρ width and the in-medium thermal distortion are taken into account.)

An analogous situation concerns the decay of the neutral kaon, $K_S^0 \rightarrow \pi^+ \pi^-$. Although less abundant than the ρ meson, the $K^0(498)$ leads to pion pairs with a smaller invariant mass but, fortunately, the corresponding pion momentum still exceeds 200 MeV/c, thus being just above the kinematical region of interest.

It should also be noted that although both $\eta(550)$ and $\omega(780)$ may contribute $\pi^+ \pi^-$ pairs, these all arise in three-body decays, which renders them only rather weakly correlated and thus they could not imitate the expected relatively narrow correlation characteristic of the signal pions.

For completeness it may be worthwhile noting that the effect should also manifest itself in electromagnetic observables, as already pointed out in Ref. [1]. One mechanism is the annihilation of charge-conjugate pion pairs, $\pi^+ \pi^- \rightarrow l^+ l^-$ and $\pi^+ \pi^- \rightarrow 2\gamma$, which may lead to an enhancement of dileptons and photons in the appropriate kinematical regimes. Another is the decay of the neutral pion, $\pi^0 \rightarrow 2\gamma$. Since the chiral antenna mechanism produces π^0 pairs in

full analogy with the $\pi^+\pi^-$ pairs, the resulting decay photons should exhibit corresponding enhancements in both their average spectrum and the associated event-by-event multiplicity fluctuation.

The mechanism responsible for creating the charge-conjugate pion pairs also manifests itself as an enhancement of the pion autocorrelation, reflecting the growing clumpiness of the multiplicity distribution brought out in Ref. [8]. In fact, according to the analysis presented in Ref. [1], the dynamically generated correlations contribute equally to the correlation between same-charge pions having similar momenta and the correlation between opposite-charge pions having opposite momenta. The resulting reduced autocorrelation function looks qualitatively similar to the charge-conjugate correlation function, apart from the shift in $\Delta\varphi$ by 180° . However, the values are generally larger and, in particular, the correlation persists for the higher energy bands. This latter feature is due to the fact that there is already an autocorrelation present in the initial Bose-Einstein quasiparticle gas as a result of the quantum-statistical fluctuations. For this reason, this observable is not exclusively generated in the course of the dynamical evolution and hence it is less suitable as a signal. Moreover, the classical field treatment employed here is expected to be less reliable for calculating the autocorrelation.

IV. CONCLUDING REMARKS

The present paper reports on more detailed studies of the recently proposed back-to-back signal in the correlation between soft charge-conjugate pions [1]. The basic effect is expected on rather general grounds and, within the linear σ model, it can be approximately understood in terms of the evolving in-medium effective pion mass, which depends both on the chiral order parameter and on the degree of agitation. The agitation is initially very large but it then subsides quickly as the collision zone disperses. Because of the high initial excitation, the chiral order parameter is expected to be reduced in magnitude, relative to its value in vacuum, f_π , and its subsequent relaxation is expected to have a nonequilibrium character reminiscent of a damped oscillator with a changing frequency. The resulting time dependence may in turn lead to pion pair production, in analogy with the production of lepton pairs by a time-dependent electromagnetic field. Since the resulting yield is sensitive to the details of the

evolution, the effect might be exploited as a probe of the relaxation dynamics, if experimentally identifiable.

In order to elucidate the effect in scenarios resembling those created in high-energy nuclear collisions, we have considered cylindrical systems that are endowed with a longitudinal Bjorken scaling expansion, Bjorken rods. The signal was found to be present at a small but significant level. It is concentrated in the soft end of the transverse spectrum and has an azimuthal dispersion of about 40° . The present calculations, based on the semiclassical linear σ model, lead to a peak value of around 8% for the reduced back-to-back correlation of charge-conjugate pion pairs.

However, the linear σ model includes only certain degrees of freedom and it significantly underestimates the total pion yield, so one would expect that a more complete treatment, yet unavailable, would yield a considerably weaker signal, the suppression being easily in excess of an order of magnitude. To this dilution comes the as yet poorly known degradation due to possible encounters between the emerging signal pions and any remaining hadrons in the environment.

Any analysis of the experimental data should, therefore, be carried out with corresponding care and may well present a challenge. Such an undertaking would nevertheless seem worthwhile because of the potential insight that could be gained. If the signal is indeed identified with sufficient significance, then its dependence on the various collision parameters could provide unique information on chiral symmetry far away from equilibrium. Conversely, should the analysis suggest that the effect is indiscernible to a sufficiently high degree of accuracy, the adequacy of the linear σ model would be in doubt and suitable revision at this basic model level would be called for. The present study thus supports the suggestion made in Ref. [1] that the data being obtained at RHIC [18] be analyzed for indications of the effect.

ACKNOWLEDGMENTS

This work was supported by the Director, Office of Energy Research, Office of High Energy and Nuclear Physics, Nuclear Physics Division of the U.S. Department of Energy under Contract No. DE-AC03-76SF00098 and by the Gesellschaft für Schwerionenforschung, Darmstadt, Germany. The author wishes to acknowledge helpful discussions with J. Klay, S. Soff, R. Vogt, X. N. Wang, and N. Xu.

-
- [1] J. Randrup, Phys. Rev. C **63**, 061901(R) (2001).
 - [2] K. Rajagopal, in *Quark-Gluon Plasma 2*, edited by R. Hwa (World Scientific, Singapore, 1995).
 - [3] J.-P. Blaizot and A. Krzywicki, Acta Phys. Pol. B **27**, 1687 (1996).
 - [4] J.D. Bjorken, Acta Phys. Pol. B **28**, 2773 (1997).
 - [5] M.M. Aggarwal *et al.*, WA98 Collaboration, Phys. Lett. B **420**, 169 (1998).
 - [6] T. Brooks *et al.*, MiniMax Collaboration, Phys. Rev. D **61**, 032003 (2000).
 - [7] J. Randrup, Nucl. Phys. A **616**, 531 (1997).
 - [8] T.C. Petersen and J. Randrup, Phys. Rev. C **61**, 024906 (2000).
 - [9] M. Bleicher *et al.*, J. Phys. G **25**, 1859 (1999); S.A. Bass *et al.*, Prog. Part. Nucl. Phys. **41**, 225 (1998).
 - [10] X.N. Wang, Phys. Rev. D **46**, 1900 (1992); Phys. Rep. **280**, 287 (1997).
 - [11] M. Bleicher, J. Randrup, R. Snellings, and X.N. Wang, Phys. Rev. C **62**, 041901(R) (2000).
 - [12] S. Jeon and V. Koch, Phys. Rev. Lett. **83**, 5435 (1999); **85**,

- 2076 (2000).
- [13] M. Asakawa, U. Heinz, and B. Müller, Phys. Rev. Lett. **85**, 2072 (2000).
- [14] S.A. Bass, P. Danielewicz, and S. Pratt, Phys. Rev. Lett. **85**, 2689 (2000).
- [15] J. Randrup, Phys. Rev. D **55**, 1188 (1997).
- [16] R.D. Pisarski, Phys. Rev. D **52**, R3773 (1995).
- [17] J. Randrup, Phys. Rev. C **62**, 064905 (2000).
- [18] See *Quark Matter 2001*, Proceedings of the 15th International Conference on Ultra-Relativistic Nucleus-Nucleus Collisions, edited by T.J. Hallman, D.E. Kharzeev, J.T. Mitchell, and T. Ullrich [Nucl. Phys. **A698** (2002)].